Proceedings of the ASME 2012 6th International Conference on Energy Sustainability &
10th Fuel Cell Science, Engineering and Technology Conference
ESFuelCell2012
July 23-26, 2012, San Diego, CA, USA

ESFuelCell2012-91246

HEAT AND MASS TRANSFER CHARACTERISTICS OF A ZEOLITE 13X/CACL$_2$ COMPOSITE ADSORBENT IN ADSORPTION COOLING SYSTEMS

K.C. Chan
Department of Mechanical Engineering,
The Hong Kong University of Science and Technology,
Kowloon, Hong Kong
meckc@ust.hk

Christopher Y. H. Chao
Department of Mechanical Engineering,
The Hong Kong University of Science and Technology,
Kowloon, Hong Kong
meyhchao@ust.hk

M. Bahrami
Mechatronic Systems Engineering,
School of Engineering Science,
Simon Fraser University,
Surrey, BC, Canada V3T 0A3
mbahrami@sfu.ca

ABSTRACT

The performance of the adsorption cooling system using the zeolite 13X/$CaCl_2$ composite adsorbent was studied using a numerical simulation. The novel zeolite 13X/$CaCl_2$ composite adsorbent with superior adsorption properties was developed in previous studies [11]. It has high equilibrium water uptake of 0.404 *g/g* between 25^{o}C and 100^{o}C under 870Pa. The system specific cooling power (SCP) and coefficient of performance (COP) were successfully predicted for different operation parameters. The simulated COP with the composite adsorbent is 0.76, which is 81% higher than a system using pure zeolite 13X under desorption temperature of 75^{o}C. The SCP is also increased by 34% to 18.4 W/kg. The actual COP can be up to 0.56 compared to 0.2 for zeolite 13X-water systems, an increase of 180%. It is predicted that an adsorption cooling system using the composite adsorbent could be powered by a low grade thermal energy source, like solar energy or waste heat, using the temperature range of 75^{o}C to 100^{o}C.

The performance of the adsorber with different design parameters was also studied in the present numerical simulation. Adsorbents with smaller porosity can have higher thermal conductivity and may result in better system performance. The zeolite bed thickness should be limited to 10mm to reduce the thermal response time of the adsorber. Addition of high thermal conductivity materials, for example carbon nanotube, can also improve the performance of the adsorber. Multi-adsorber tube connected in parallel can be employed to provide large heat transfer surface and maintain a large SCP and COP. The desorption temperature also showed a large effect on the system performance.

INTRODUCTION

Along with rapid development of modern society, energy demand rises in wide range of sectors from our daily usages to industrial applications. High energy consumption has become a worldwide problem. According to U.S. Department of Energy, total worldwide primary energy consumption was 520 EJ in 2008 while it was 400 EJ in 1998 and 360 EJ in 1988 [1]. It is predictable that the demand on energy will not be reduced and will increase continuously along with the rapid development of the cities all over the world. In many places, air-conditioning is a daily necessity but it also contributes significantly to electricity consumption - 183 billion kWh, or 16% of electricity consumption by U.S. households, for example [2]. In 1997, 72.5% of homes in the U.S. were equipped with air conditioning, and the figure has been increasing [3]. Air conditioning systems play an even more important role in regions with higher average ambient temperatures and humidity. For example, it contributes up to 40 – 50% of the total building electricity consumption in Asian metropolitan cities such as Hong Kong [4].

To ease the problems of energy shortage, adsorption cooling systems (ACS)s can be a good alternative. ACS offers a number of distinct advantages, as ACS is an environmentally-friendly thermal system where low grade thermal energy, e.g. solar energy or waste heat from industrial processes, boilers in hospitals and hotels, commercial kitchens, etc., can be used as the input energy source. The working principle and shortages of ACSs have been described in many literatures, see for example [5 – 10]. Major challenges facing the commercialization of ACS include low thermal conductivity and low uptake capacity of the currently available adsorbents, which lead to low specific cooling capacity (SCP) and low coefficient of performance (COP), which in turn lead to bulky and inefficient ACS.

NOMENCLATURE

a_i	i = 0 – 3, Numerical constants in Equation (1)
b_i	i = 0 – 3, Numerical constants in Equation (1)
c_p	specific heat capacity (J/kg.K)
d_p	average diameter of adsorbent particle (m)
h_{ad}	heat of adsorption (J/mol)
Δh_a	isosteric enthalpy of adsorption (J/mol)
$h_{fg,water}$	heat of vaporization of water (kJ/kg)
k	thermal conductivity (W/mK)
K	adsorption rate coefficient (1/s)
k_1	empirical constant used in Equation (3) (1/s)
k_2	empirical constant used in Equation (3) (1/K)
L	Length of the adsorbent bed (m)
m	total mass of the tested sample (g)
$\dot{m}_{ad}$	adsorption rate (g/g.s)
P	pressure (Pa)
Q	power (W)
R	universal gas constant (J/molK), or radius (m)
T	temperature (K)
u_g	flow velocity of the adsorbate vapor in the z direction (m/s)
U_m	mean velocity of the HTF flow (m/s)
v_g	flow velocity of the adsorbate vapor in the r direction (m/s)

Greek symbol

ε	adsorbent bed's porosity
μ	dynamic viscosity (kg/m.s)
ρ	density (kg/m^3)
ω	water uptake (g/g)

Abbreviation

COP	Coefficient of performance
SCP	Specific cooling power (W/kg)

Subscripts

ad	adsorption
c	condenser
de	desorption
e	evaporator
eq	equilibrium for ω, equivalent for k
f	heat transfer fluid (HTF)
g	water vapor
H	heat source
m	copper tube
z	adsorbent

To improve the COP and SCP of ACS, a novel zeolite 13X/$CACl_2$ composite adsorbent with superior adsorption properties was developed in previous studies [11]. It has high equilibrium water uptake of 0.404 *g/g* between 25°C and 100°C under 870 *Pa*, which was 295% and 320% of that of zeolite 13X and silica gel, respectively, as shown in Figure 1.

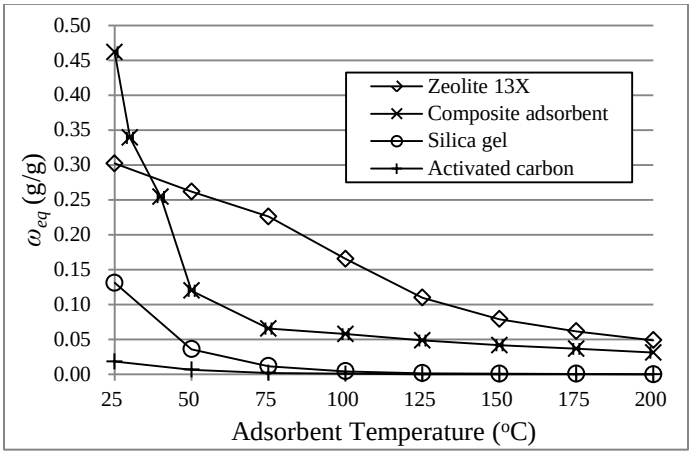

Figure 1. Equilibrium water uptake of zeolite13X/$CaCl_2$ composite adsorbent, zeolite 13X, silica gel and activated carbon. All data at 870Pa pressure

With the composite adsorbent developed, detailed numerical simulations were carried out to predict the performance of an ACS utilizing the zeolite 13X/$CaCl_2$ composite adsorbent. Heat and mass transfer models were developed to assist the optimization of the system prototypes design in order to maximize COP and SCP. Adsorption kinetics, varying heat of adsorption, adsorbate flow inside adsorbent bed, the flow pattern of the heat transfer fluid, which have not been fully addressed in many previous studies, were considered. The result was compared with that of a system using conventional zeolite 13X in terms of COP and SCP. Simulation on the system operation cycles was also conducted under various operation conditions to study the effects of changing different cycle parameters.

MATHEMATICAL MODELING

The heat and mass transfer inside an adsorber is a complex problem with many different mechanisms involved. It is also a multi-phase problem with vapor, adsorbed and solid states present. The design of the adsorber can largely affect the overall performance of the whole system. An adsorber model was therefore constructed in an attempt to predict the performance of full scale adsorbers. The configuration of the model adsorber is shown in Figure 2. It has a copper tube in the middle. Heat transfer fluid (HTF) could flow through the tube from the heat source or sink. A layer of adsorbent was coated on the copper tube. A cover was used to maintain the low pressure inside the adsorber. There was a small separation of the cover from the adsorbent for water vapor to enter and leave the adsorber. Water vapor could pass under the cover freely to the adsorbent. A complete cycle including adsorption and desorption phases could be modeled with this system. A cylindrical coordinate system with time dependence (r, z, θ, t) was used for the numerical simulation. The volume simulated is enclosed by a dashed line in Figure 2. It was assumed that no heat or mass was transferred in the θ direction because of the axial symmetry of the adsorber, i.e. $(r, z, \theta, t) \rightarrow (r, z, t)$. There was no dead air volume, so the volume inside the connecting tubes and other empty spaces was small.

Table 1. Parameter values and operating conditions simulation

Name	Symbol	Value
Mean flow velocity of the HTF flow	U_m	0.1 m/s
Evaporator pressure	P_e	872.5Pa
Condenser pressure	P_c	12352Pa
Desorption Temperature	T_{de}	473 K for zeolite 13X, 348 K for composite adsorbent
Adsorption Temperature	T_{ad}	313 K
Copper tube inner radius	rf	0.009 m
Copper tube outer radius	Rf	0.01 m
Adsorbent layer outer radius	Rz	0.025 m
Adsorbent layer length	L	0.5 m
Numerical constant for zeolite 13X	a_i	0: 13.4167; 1: 1.1197; 2: -73.205×10^{-3}; 3: 1.7211×10^{-3}
	bi	0: -7373.04; 1: 67.3361 2: 0.56291; 3: -3.5003×10^{-3}
Numerical constant for composite adsorbent	ci	0: 381.4; 1: -3.463; 2: 0.01008; 3: -9.153×10^{-6}(for adsorption) 0: 400.8; 1: -3.532; 2: 0.01002; 3: -8.908×10^{-6}(for desorption)
Density of the HTF	ρ_f	$3\times10^{-7}T^3+0.0018T^2-2.1915T+1282.9$ kg/m3
Specific heat capacity of the HTF	$c_{p,f}$	$6\times10^{-7}T^3-0.0002T^2$ +1.7939T+1862.5 J/kgK
Thermal conductivities of the HTF	k_f	$2\times10^{-10}T^3-5\times10^{-7}T^2$ +0.0002T+0.1008W/mK
Density of the adsorbent	ρ_z	1100 kg/m3
Specific heat capacity of the adsorbent	$c_{p,z}$	836 J/kgK
Thermal conductivities of the adsorbent	k_z	0.2 W/mK
Adsorbent bed porosity	ε	0.3
Pre-exponent constant of surface diffusivity	D_0	3.92×10^{-6} m^2/s
Activation energy of surface diffusion	E_d	28035 J/mol
Adsorbent particle diameter	d_p	2×10^{-6} m
Specific heat capacity of the adsorbed water	$c_{p,ad}$	4186.8 J/kgK
Specific heat capacity of the adsorbate in gas state	$c_{p,g}$	$(-3.595\times10^{-9}T^3+1.055\times10^{-5}T^2$ $+0.1923\times10^{-2}T+32.24)/M$ J/kgK
Molar mass of the adsorbate gas	M	18.01528 g/mol
Thermal conductivities of the water vapor	k_g	$3\times10^{-8}T^2+5\times10^{-5}T+0.0006$ W/mK
Viscosity of water vapor	μ_g	$(0.0361T-1.0108)\times10^{-6}$ $kgm^{-1}s^{-1}$

The values of the basic parameters used are listed in Table 1. The desorption temperature changes with the use of adsorbent. It was set to be 200°C for zeolite 13X and 75°C for composite adsorbent. Under these desorption temperatures, the adsorbents can be almost totally desorbed. The adsorption temperature is set to be slightly higher than room temperature 40°C, which is about the temperature of an air-conditioner placed outdoor with shield in summer. The base size of the copper tube was chosen to near to half inch which is a very common copper tube size. 10mm was used because it is more convenient for simulation. The performance of the composite adsorbent was compared with zeolite 13X. Some design parameters, including zeolite bed thickness, length and desorption temperature were changed in the simulation model to find out the optimized design and zeolite 13X and water pair was employed. The simulation conditions are listed in Table 2. The analytical model of each of the mechanism was discussed in detail.

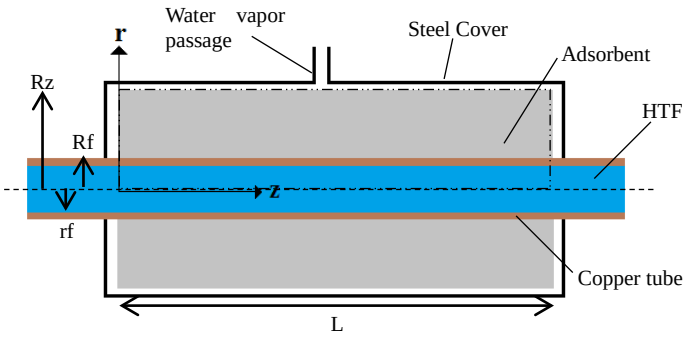

Figure 2. Cross section of the model adsorber and the area to be simulated (circled with a dashed line)

Table 2. The design parameters of the adsorber used in the simulation model

	T_H	T_L	R_z	L	dr	dz
SET 1	200	40	**0.03**	0.5	0.0025	0.05
SET 2	200	40	**0.02**	0.5	0.0025	0.05
SET 3	200	40	**0.015**	0.5	0.0010	0.05
SET 4	200	40	**0.013**	0.5	0.0005	0.05
SET 5	200	40	**0.011**	0.5	0.0005	0.05
SET 6	200	40	0.015	**1**	0.0010	0.1
SET 7	200	40	0.015	**2**	0.0010	0.2
SET 8	200	40	0.015	**4**	0.0010	0.4
SET 9	200	40	0.015	**8**	0.0010	0.8
SET 10	**150**	40	0.015	4	0.0010	0.4
SET 11	**250**	40	0.015	4	0.0010	0.4
SET 12	**300**	40	0.015	4	0.0010	0.4

Equilibrium water uptake, adsorption rate and heat of adsorption

The equilibrium water uptake on the zeolite 13X was correlated using the linear driving force model [12] such that

$$\ln P = a(\omega_{eq}) + b(\omega_{eq}) \Big/ T_z$$
$$a(\omega) = a_0 + a_1\omega_{eq} + a_2{\omega_{eq}}^2 + a_3{\omega_{eq}}^3 \quad (1)$$
$$b(\omega) = b_0 + b_1\omega_{eq} + b_2{\omega_{eq}}^2 + b_3{\omega_{eq}}^3$$

where P is pressure and a_i (i = 0–3) and b_i (i = 0–3) are numerical constants found by curve fitting. For the composite adsorbent, however, there is still not enough experimental data to employ in this model. The equilibrium water uptake on the composite adsorbent was correlated using

$$\omega_{eq} = 1\Big/\left(c_0 + c_1T_z + c_2T_z^2 + c_3T_z^3\right) \quad (2)$$

where c_i (i = 0–3) are numerical constants found by curve fitting. The curve fitting was done by nonlinear least squares method with trust-region algorithm. The values of R-square and sum of squared errors of the fittings were higher than 0.985 and smaller than 0.003, respectively. The adsorption rate was also modeled using linear driving force model simplified [13] to:

$$\frac{d\omega}{dt} = \dot{m}_{ad} = k_1 \exp\left(-\frac{k_2}{T_z}\right)(\omega_{eq} - \omega) = K(\omega_{eq} - \omega), \quad (3)$$
$$K = k_1 \exp\left(-\frac{k_2}{T_z}\right)$$

where k_1 and k_2 are to be determined experimentally and K is a function of temperature only. During adsorption, the adsorbate vapor was changed to an adsorbed state with physical properties similar to its liquid state. The heat of adsorption was released during adsorption. The adsorption heat for a specific amount of adsorbate adsorbed, ω_a, can be calculated from the equilibrium between the chemical potential of the vapor and the adsorbent [14]. The Clausius-Clapeyron equation was used to develop the equilibrium chemical potential [15] as

$$\left(\frac{\partial \ln P}{\partial T}\right)_{\omega_a} = -\frac{\Delta h_a}{RT^2} = \frac{h_{ad}}{RT^2} \quad (4)$$

where h_{ad} can be assumed to be independent of temperature [16]. With this assumption, Equation (4) can be integrated to

$$(\ln P)_{\omega_a} = -\frac{h_{ad}}{RT} + C\,. \quad (5)$$

Comparing Equation (1) with Equation (4), $a(\omega)$ is constant when $\omega = \omega_a$, so

$$h_{ad}/R = -b(\omega_{eq}) = -\left(b_0 + b_1\omega_{eq} + b_2{\omega_{eq}}^2 + b_3{\omega_{eq}}^3\right) \quad (6)$$

Hence the heat of adsorption depends on the amount of water adsorbed and does not depend on temperature. Besides the linear driving force model, another empirical relationship between water vapor pressure, adsorbent temperature and equilibrium water uptake was documented by Dini and Worek [17]. This approach has a larger freedom to correlate the experimental results with heat of adsorption. Thus, this approach and the linear driving force model will be utilized to

investigate the properties of the composite adsorbent in detail in future work after more experimental result was obtained.

Energy and mass conservation equations

After formulating the model of the adsorption process, energy conservation equations were formulated for the HTF, the copper tube and the adsorbent. The HTF flow has often been modeled as uniform with no temperature gradient in the flow [18, 19], but the flow should then be slow if solar heat or waste heat is used as the heat source. The mean HTF flow velocity, U_m, was set to be 0.1m/s. The kinematic viscosity, υ, is in the range of 1.1 to 10 cSt. The Reynolds number was calculated to be in the range of 200 to 1800, which indicates laminar flow. It was also assumed that the tube was long enough that the flow was fully developed. The energy equation for fully developed laminar flow inside a circular pipe [20] could then be used. Convective and conductive heat transfers in the HTF flow were assumed. Only conduction was assumed in the copper tube.

Since heat and mass transfer occurs during both adsorption and desorption, mass change, mass diffusion, heat conduction and heat generation in the adsorbent bed are given by [21]:

$$\left(\rho_z c_{p,z} + \omega\rho_z c_{p,ad} + \varepsilon\rho_g c_{p,g}\right)\frac{\partial T_z}{\partial t} + u_g \rho_g c_{p,g}\frac{\partial T_z}{\partial z} + v_g \rho_g c_{p,g}\frac{\partial T_z}{\partial r} = k_{eq}\left(\frac{\partial^2 T_z}{\partial z^2} + \frac{\partial^2 T_z}{\partial r^2} + \frac{1}{r}\frac{\partial T_z}{\partial r}\right) + \rho_z h_{ad}\frac{\partial \omega}{\partial t} \quad (7)$$

There was space between the adsorbent particles, so the equivalent thermal conductivity of the adsorbent bed was estimated using modified Zehner-Schlunder model [22]:

$$\frac{k_{eq}}{k_g} = \left(1-\sqrt{1-\varepsilon}\right) + \frac{1-\sqrt{\varepsilon}}{\lambda} + \left(\sqrt{1-\varepsilon}+\sqrt{\varepsilon}-1\right)\left[\frac{b(1-\lambda)}{(1-\lambda b)^2}\ln\frac{1}{\lambda b} - \frac{b-1}{1-\lambda b}\right], \quad (8)$$

$$b = \left(\frac{1-\varepsilon}{\varepsilon}\right)^{0.9676}, \quad \lambda = \frac{k_g}{k_z}.$$

Mass conservation in the adsorbent bed yields

$$\varepsilon\frac{\partial \rho_g}{\partial t} + \nabla\cdot\left(\rho_g \vec{u}_g\right) + \rho_z\frac{\partial \omega}{\partial t} = 0. \quad (9)$$

The adsorbent bed is a porous medium, so water vapor passes through the bed following Darcy's law [19] with the velocity vector

$$\vec{u}_g = -\frac{K_{ap}}{\mu_g}\nabla P,\ K_{ap} = \frac{d_p^2\varepsilon^3}{150(1-\varepsilon)^2}. \quad (10)$$

COP and SCP

The system performance was quantified in terms of its COP and SCP. The power supplied to the system was calculated as

$$Q_H = -\int_0^L 2\pi R_f k_{eq}\left.\frac{\partial T_z}{\partial r}\right|_{r=R_f} dz, \quad (11)$$

which is the heat supplied from the HTF to the adsorbent. The total energy supplied is

$$E_{\sup ply} = \int_0^{t_{de}} Q_H dt, \quad (12)$$

where t_{de} is the duration of desorption. The cooling power of the system is

$$Q = m_z \dot{m}_{ad} h_{fg,water}. \quad (13)$$

Similar to the total energy supplied, the total cooling power is

$$E_{cooling} = \int_0^{t_{ad}} Q dt, \quad (14)$$

where t_{ad} is the duration of adsorption. The system's COP and SCP are thus

$$COP = \frac{E_{cooling}}{E_{\sup ply}} \text{ and } SCP = \frac{E_{cooling}}{(t_{ad}+t_{de})m_z}. \quad (15)$$

Initial and boundary conditions

The presence of the other gases can largely suppress the mass transfer of the gaseous adsorbate. This suggests that the presence of other gases in the adsorber should be prevented, so the adsorber must be evacuated before filing the water vapor. The total pressure inside the adsorber should be equal to the water vapor pressure inside. The simulation was started from the adsorption phase that the adsorber was just desorbed and connected to the condenser. Thus, the initial temperature of the zeolite, the copper tube and the HTF are the desorption temperature, and the initial pressure inside the zeolite bed is equal to the condenser pressure, P_c, and the condenser pressure was set to be the saturation pressure of water at 50°C. The water uptake of the zeolite is equal to the equilibrium water uptake under desorption temperature and condenser pressure:

$$T_z(r,z,0) = T_m(r,z,0) = T_f(r,z,0) = T_H,$$
$$P(r,z,0) = P_c,\ \omega(r,z,0) = \omega_{de}. \quad (16)$$

For t > 0, the temperature of the HTF inlet is set to be the desired adsorption/ desorption temperature,

$$T_f(r,0,t) = \begin{cases} T_L & \text{during adsorption} \\ T_H & \text{during desorption} \end{cases} \quad (17)$$

In the interfaces between the HTF and the copper tube, and between the copper tube and the zeolite bed, the temperature is assumed to be the same,

$$T_f(r_m,z,t) = T_m(r_m,z,t),\ T_m(R_m,z,t) = T_z(R_m,z,t). \quad (18)$$

The temperature gradients in the *r*- direction are also the same,

$$\left.\frac{\partial T_f}{\partial r}\right|_{r=0} = 0,\ k_f\left.\frac{\partial T_f}{\partial r}\right|_{r=r_m} = k_m\left.\frac{\partial T_m}{\partial r}\right|_{r=r_m},\ k_m\left.\frac{\partial T_m}{\partial r}\right|_{r=R_m} = k_z\left.\frac{\partial T_z}{\partial r}\right|_{r=R_m}. \quad (19)$$

On the sides of the zeolite bed, the temperature gradients are zero by assumed that there is no heat transfer from the sides to outside. The pressure gradients are also zero between the copper tube and adsorbent,

$$\left.\frac{\partial T_m}{\partial z}\right|_{z=0} = \left.\frac{\partial T_m}{\partial z}\right|_{z=L} = \left.\frac{\partial T_z}{\partial z}\right|_{z=0} = \left.\frac{\partial T_z}{\partial z}\right|_{z=L} = \left.\frac{\partial T_z}{\partial r}\right|_{r=R_z} = \left.\frac{\partial P_z}{\partial r}\right|_{r=R_m} = 0. \quad (20)$$

During adsorption, the pressure in the adsorbent is equal to the pressure in the evaporator, which is the saturation pressure of water at 5°C. During desorption, it is equal to the pressure in the condenser, which is the saturation pressure of water at 50°C,

$$P(R_z, z, t) = P(r, 0, t) = P(r, L, t) = \begin{cases} P_e \text{ during adsorption} \\ P_e \text{ during desorption.} \end{cases} \quad (21)$$

NUMERICAL SIMULATION

Finite difference method was employed to construct the simulation program. The differential equations were first converted to finite difference form using second-order finite difference approximations [23]. The alternating-direction implicit (ADI) method was used to split different directions into difference simulation steps [24]. Compared to other numerical methods like the Crank-Nicolson method, the ADI method is more convenient to apply. In Crank-Nicolson method, the changes in different directions with respect to time are all mixed in a single step. Large matrices are needed to be solved. This requires a large computational power and is very time consuming. By using ADI method, trial and error operation can be employed with each equation in calculating the values in the next time step. The time step was cut into two half steps. In each half time step, the changes in one direction were considered. By specifying a conscientious convergence criterion, for example 10^{-6}, the error induced in the calculation can be minimized. The ADI method is also unconditionally stable and has small truncation errors in the order of O [$(\Delta t)^2$, $(\Delta x)^2$, $(\Delta y)^2$]. Time steps of variable duration were used to increase the speed of the simulation while maintaining good accuracy. First, the simulations were conducted in the time step of 10^{-4} s to account for the relatively large finite differences in each node and differences between initial values and calculation results in the beginning of the simulations. When the simulation continued, the finite differences, especially pressure gradient, were reduced. The time steps were gradually increased to 0.1s for faster simulation. The simulation results in each different size of time step were inspected to check if there were any abnormal outcomes. The grid size was also changed for different simulated adsorber sizes to have enough resolution and reasonable simulation time. Finer grid has a higher resolution but the simulation time will be largely increased. Majority of the simulation has 150 nodes or above.

RESULTS AND DISCUSSION

System performance prediction

The adsorption-desorption cycles adsorbers using pure zeolite 13X and the zeolite 13X/ $CaCl_2$ composite adsorbent were simulated. The equilibrium water uptake of the adsorbents at 870Pa and at atmospheric pressure is shown in Figure 3 from 25°C to 200°C. The shape of curve for composite adsorbent in Figure 3 is very different from zeolite 13X because of the presence of $CaCl_2$ in the composite adsorbent. The equilibrium water uptake of $CaCl_2$ decreases sharply from more than 0.8 *g/g* to 0.1*g/g* when temperature increases from 25°C to 70°C. The composite adsorbent is also clearly less dependent on pressure, as the difference between the curves under 870Pa and room pressure is much smaller for the 13X/ $CaCl_2$ composite adsorbent which is good in an ACS where adsorption takes place at low pressure and desorption takes place under higher pressure. Figure 4 shows the variation of the average water uptake with the temperature of the adsorbent bed. The difference in water uptake between the adsorption phase and desorption phase is larger for the system using the composite adsorbent, as previously discussed. The cycle time of the system using the composite adsorbent is slightly shorter than that using pure zeolite 13X. This is because the composite adsorbent requires a lower desorption temperature. The COP and SCP of the two adsorbers are shown in Table 3. The COP of the system using the composite adsorbent is 0.76, which is 81% better than the system using pure zeolite 13X. The SCP is also increased by 35% to 18.4 W/kg. The reason is that the larger difference in water uptake for the composite adsorbent provides more total cooling energy. With almost no change in cycle time, the SCP is increased. The lower desorption temperature for the composite adsorbent reduces the thermal energy needed to heat up the adsorbent for desorption. Hence, the COP is greatly increased. The system with the composite adsorbent also performs better than a system using selective water sorbent (SWS) [25]. SWS was synthesized from silica gel, which is another commonly used adsorbent and it was reported to have a very high equilibrium water uptake, 0.7g/g. This material also has a high potential to be used in ACS. A system using SWS has a COP of 0.52 and a SCP of 20W/kg with similar conditions, including operation temperatures and pressure, by experiment and simulation. The composite adsorbent is 46% better than SWS in terms of COP, though 8% worse in terms of SCP. The SCP of the system using the 13X/$CaCl_2$ adsorbent is lower because the COP was maximized in the simulation and a lower desorption temperature was selected to demonstrate the usefulness of the 13X/$CaCl_2$ adsorbent in solar powered ACSs where the temperature of the heat source may be low. If the desorption temperature were changed to 100°C, the COP and SCP of the system would be 0.65 and 22 W/kg respectively.

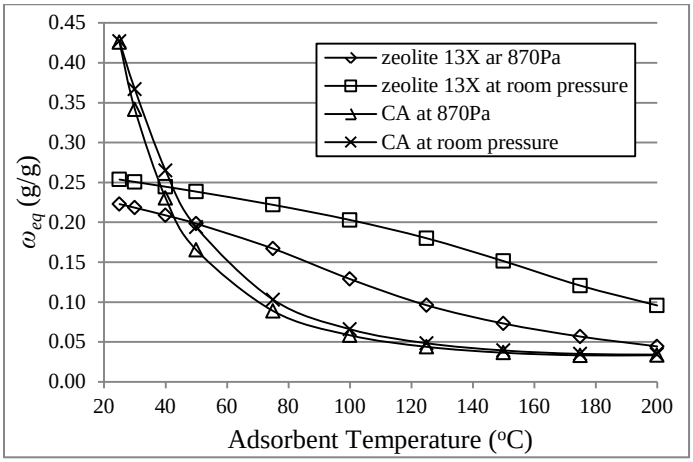

Figure 3. Equilibrium water uptake of the zeolite 13X/$CaCl_2$ composite adsorbent (CA) and pure zeolite 13X at 870Pa and atmospheric pressure

Table 3. Simulated system COP and SCP of an ACS using pure zeolite 13X, zeolite 13X/$CaCl_2$ composite adsorbent and SWS

	Pure zeolite 13X	Zeolite 13X/ $CaCl_2$ composite adsorbent	SWS [18]
COP	0.42	0.76	0.52
SCP (W/kg)	13.7	18.4	20

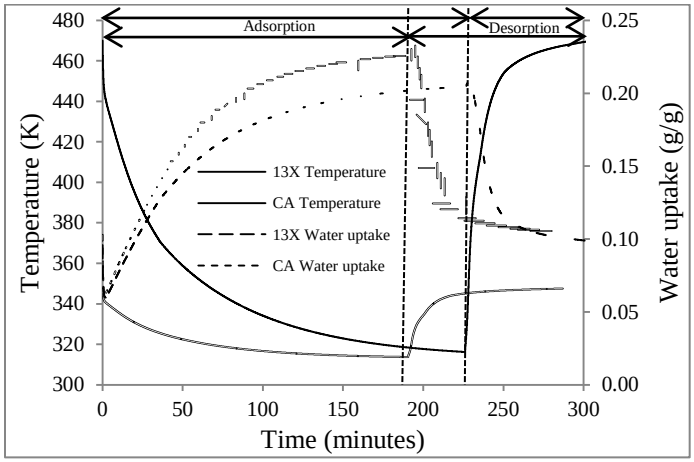

Figure 4. Adsorbent temperature and water uptake in the adsorber during simulation of zeolite 13X and composite adsorbent (CA)

Unwanted heat is lost to the surroundings when the adsorbent is heated for desorption and electricity is supplied to operate the valves and other electrical components in a real system. This energy is lost in every cycle and cannot be recovered. Using the 13X/$CaCl_2$ composite adsorbent instead of zeolite 13X can reduce the number of cycles and lower the desorption temperature, and this can greatly reduce the total heat loss from the system and the electricity consumed by the various electrical components. This would further increase the disparity in actual COP between systems using the zeolite 13X/CaCl2 composite adsorbent and zeolite 13X. The degree of improvement depends on specific parameters of each system, and the improvement is larger for a system with larger heat loss to the surroundings in each cycle. The ideal COP of the zeolite 13X-water pair is about 0.54, but the actual COP of a system without treatment of waste heat is less than 0.2 [26]. So the energy loss is twice that of an ideal system. A 320% improvement in $\Delta\omega$ should increase the cycle time by 320% and thus decrease heat losses. The actual COP using the 13X/$CaCl_2$ composite adsorbent is predicted to be 0.56, which is a 180% improvement over using zeolite 13X. For purposes of comparison, the COP of a system using $CaCl_2$-in-silica-gel was estimated to be 0.42–0.45 [18]. The zeolite 13X/$CaCl_2$ composite should thus perform better than a silica gel based system in adsorption cooling.

Effects of changing different adsorber design parameters

The design of the adsorber can affect the performance of the system. The adsorption time, desorption time, total time, mass of zeolite, water uptake during adsorption, cooling energy, cooling power, total heat supplied for desorption, SCP and COP are all listed in Table 4. Zeolite 13X/ water pair was used in this part of study because of the availability of properties and time limitation. Similar trends should be applicable for the 13X/$CaCl_2$ composite adsorbent and other adsorbents. The effects of each parameter were discussed below.

Effect of gas phase diffusion in the zeolite bed

Figure 5 shows the average pressure of the zeolite bed of condition set 1 in the first 10ms. It can be seen that the pressure decreased very fast in the beginning because the pressure in the adsorber is high, 12,352 Pa. After the adsorbent bed is connected to evaporator, the pressure decreases to 872.5 Pa which is only 7% of the initial value. This large difference in pressure drives the water vapor out from the porous zeolite bed quickly. Since there is no other gas inside, there is no diffusion barrier for the water vapor to diffuse. The transition time of pressure change is much shorter than the total adsorption time, 0.01 second comparing to 30 minutes. During adsorption, the pressure in the adsorber is about 825 Pa to 870 Pa. The difference between the simulated pressure and the evaporator pressure is only about 5%. It is suggested that mass transfer in the adsorbent bed is much faster than heat transfer. The system performance can be improved by compressing the adsorbent to decrease its porosity. This not only improves the thermal conductivity of the adsorbent bed, but also reduce the size required for the adsorber.

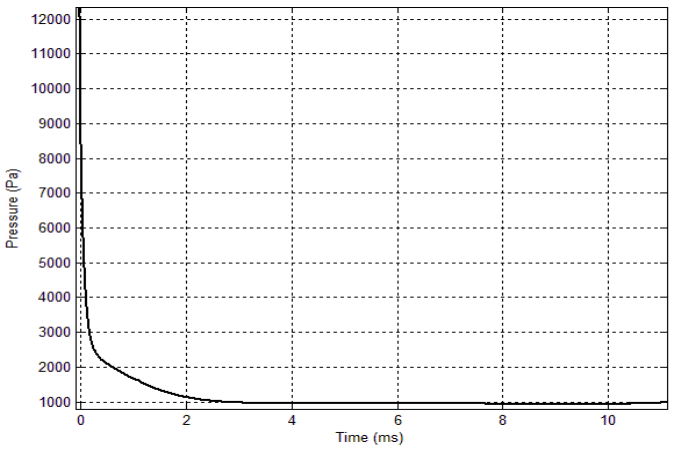

Figure 5. The simulated variation of average zeolite bed pressure for condition set 1

Adsorbent bed thicknesses

The effect of changing the zeolite bed thickness is shown in Figure 6. The cooling power increases with the zeolite bed thickness. After reaching a maximum value, it decreases with thicker zeolite bed. When there was only a thin layer of zeolite, the total mass of the zeolite was low. The zeolite bed was

Table 4. Simulation results of the 12 sets of simulation conditions

	Adsorption (min)	Desorption (min)	Total time (min)	Mass of adsorbent(g)	Water adsorbed (g)	Cooling energy (kJ)	Cooling power (W)	Total Heat - Desorption (kJ)	SCP (W/kg)	COP
SET 1	367	133	500	1382	147.8	368	12	1035	8.9	0.36
SET 2	94	52	145	518	55.4	138	16	345	30.6	0.40
SET 3	31	15	46	216	23.1	57.5	21	176	97.1	0.33
SET 4	29	5	34	119	12.7	31.7	15	120	129.9	0.26
SET 5	35	2	37	36	3.9	9.66	4	31	119.9	0.31
SET 6	32	19	51	432	46.2	115	38	405	87.8	0.28
SET 7	34	23	57	864	92.4	230	67	921	78.0	0.25
SET 8	38	27	65	1728	184.7	460	118	2023	68.5	0.23
SET 9	43	34	77	3456	369.4	920	199	4261	57.7	0.22
SET 10	36	28	63	1728	86.7	216	57	1418	32.9	0.15
SET 11	39	22	61	1728	240.3	598	162	2441	93.9	0.25
SET 12	40	20	60	1728	274.0	682	191	2752	110.3	0.25

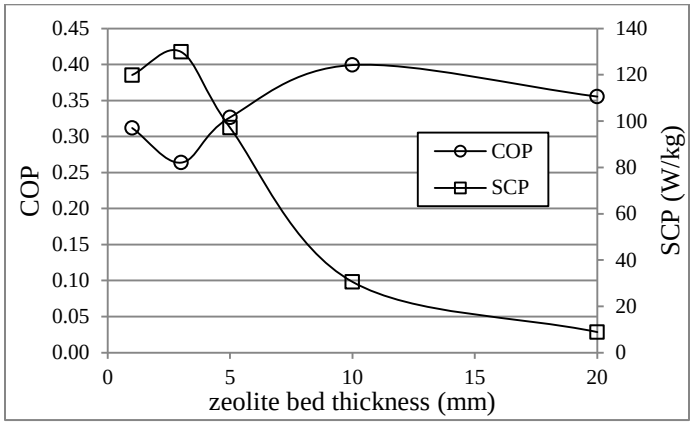

Figure 6. The effect of changing the zeolite bed thickness on the system COP & SCP

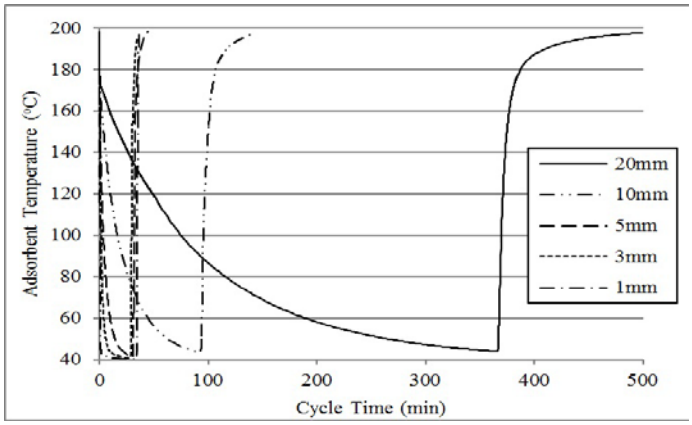

Figure 7. The average temperature profile of different zeolite bed thickness

saturated by the water vapor easily that not much cooling effect can be provided. When there was more zeolite, i.e. thicker bed, the cooling power increased. But the increased thickness increased the thermal resistance. The zeolite bed needed a long time to cool down as shown in Figure 7. The increase in the total cycle time became apparent when the thickness is larger than or equal to 10mm. The cycle time of the zeolite bed with the thickness of 20mm was about 10 times longer than that with the thickness of 3 or 5mm. The increased mass for the thicker zeolite bed was also taken into account in the system SCP. The SCP decreases sharply when the thickness is larger than 3mm, in Figure 6. A similar trend was also found for the COP. A maximum value was recorded when the bed thickness was 10mm.

This strongly suggests that the zeolite layer cannot be too thick to lower the thermal resistance. The thickness should be limited to 10mm. Methods to increase the contact area between the metal support and the zeolite should be considered. The most straight forward way is to use finned tube. If the fins were designed to be separated less than 10mm, the problem associated with the poor thermal conductivity of the zeolite can be solved. However, the addition of metal fins will also increase the thermal mass of the adsorber. The thermal response time of the adsorber will increase and the energy required to heat the adsorber to the desorption temperature will also increase. This may have negative effects on SCP and COP. Another way to solve the problem is to consolidate high thermal conductivity material with the zeolite to increase the bed thermal conductivity so the thickness of the bed can be increased. Compared to metals, carbon nanotube (CNT) has a high thermal conductivity of about 6,000W/mK under room temperature, which is 30,000 times higher than zeolite 13X and 17 times higher than pure copper [27]. The addition of CNT can fill up the empty spaces between the composite zeolite

molecules to increase the overall thermal conductivity. CNT not only has high thermal conductivity, but also has a much lower volumetric heat capacity, 0.662 J/cm^{3}K, where the value of copper is 3.442 J/cm^{3}K [28]. This shows that the thermal response of CNT is faster. The particle size of the composite adsorbent is around 2μm [11]. There are many small empty spaces between the adsorbent particles. The tiny CNTs can fill in the empty spaces and the $CaCl_2$ in the composite adsorbent and will act as a binder to hold the zeolite molecules and CNT together in order to reduce the contact resistance and enhance the overall thermal conductivity. Besides, CNT is also a porous material that water can be adsorbed in the confined space within the nanotubes [29, 30]. Adding CNTs can increase the volumetric water adsorption capacity of the composite adsorbent. Thus, adding CNTs can increase the thermal conductivity and the adsorption capacity of the composite adsorbent.

Adsorbent bed lengths

The cooling power was increased with the zeolite bed length almost linearly. It is because the cooling energy provided was directly proportional to the mass of the zeolite so as to the length of the zeolite bed. The change in cycle time for different bed lengths was small comparing to the increase in cooling energy. The change in cycle time showed its effect on the SCP, in Figure 8. The increase in cooling power was overcome by the increase in the mass of zeolite and cycle time. It was suggested that the HTF became cooler when it passed through the long copper tube and lost thermal energy to the zeolite through convection. The zeolite near the end of the copper tube required a longer time to receive enough thermal energy to reach the required desorption temperature. This lengthened the cycle time and reduced the SCP. It was also shown that the increase in bed length reduced the COP similar to the effect on the SCP. Thus, it is suggested that the length of the zeolite bed should not be too long. However, more zeolite was required to provide a larger cooling power. The best solution to this problem is to use multi-adsorber tube connected in parallel, so the length of each tube can be reduced and more zeolite can be used. Another way to minimize the effect of the increase in bed length is to increase the flow rate of the HTF. This can reduce the temperature difference between the HTF in inlet and outlet so the zeolite in every location can be heated up more simultaneously.

Desorption temperatures

The cooling power increased with the increasing desorption temperature because the difference in water uptake between the adsorption and desorption phase increases with temperature increased. The larger difference in water uptake between the adsorption and desorption phase provided a higher cooling energy for the system. The cycle times for different desorption temperatures were almost unchanged, so a higher desorption temperature can increase the cooling power of the system. An

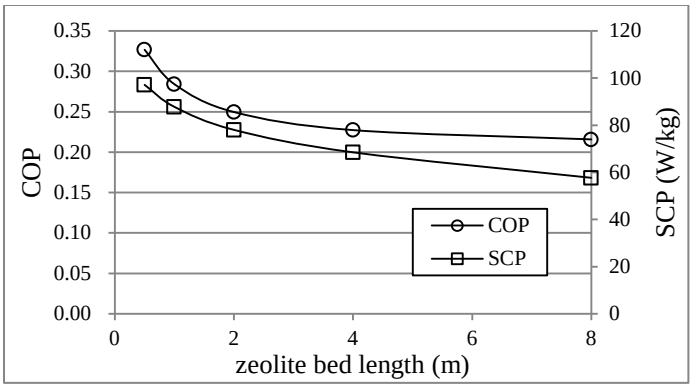

Figure 8. The effect of changing the zeolite bed length on the system COP & SCP

identical result is also shown in the SCP as in Figure 9 because the mass of the zeolite was the same for all cases. The COP was increased with the desorption temperature but the increase became very small when the desorption temperature was higher than 200^{o}C. This is because more energy was required to heat up the zeolite to the higher desorption temperature and eliminate the effect of the increased cooling power. From the results, it was suggested that the desorption temperature should be high in order to get the highest SCP. If the system COP and is the main interest, the desorption temperature should be low because high desorption temperature will increase the heat loss to the surrounding and decrease the system COP in real applications.

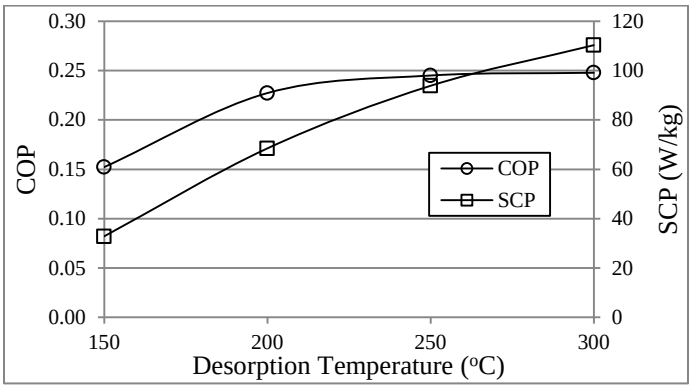

Figure 9. The effect of the desorption temperature on the system COP & SCP

CONCLUSIONS

In previous studies, the novel zeolite 13X/$CaCl_2$ composite adsorbent was developed. Numerical simulation was conducted to study the performance of the ACS using this composite adsorbent. This simulation model successfully predicted the system SCP and COP for different operation parameters. Simulation results suggest that the COP of a cooling system using the composite adsorbent would be 0.76, which is 81% better than a system using pure zeolite 13X. The SCP is also increased by 34% to 18.4 W/kg. The actual COP can be up to 0.56 compared to 0.2 for zeolite 13X-water systems, an

increase of 180%. Desorption for the 13X/$CaCl_2$ composite adsorbent can also be completed at about 75°C to 100°C, so low grade thermal energy like solar energy can be used as the energy source for this system. An ACS using this 13X/$CaCl_2$ composite zeolite has good potential for replacing vapor compression chillers to produce chilled water for central air conditioning systems.

From the simulation result, the water vapor diffusion in the adsorbent bed only has a small effect on the overall performance of the adsorber because the porosity assumed is high. It was suggested that the adsorbent bed can be compressed to have a higher density. It was also shown that the zeolite bed thickness should be limited to 10mm to reduce the bad effect caused by the poor thermal conductivity of the adsorbent. High thermal conductivity material, for example carbon nanotube, additive to increase the thermal conductivity of the zeolite bed was proposed. The prolonging of the length of the zeolite bed has negative effect on the system SCP and COP. It was proposed that multi-adsorber tube connected in parallel can be employed to provide enough cooling power and at the same time maintain a large SCP and COP. The desorption temperature was also studied and showed a large effect on the system performance. A higher desorption temperature resulted in higher SCP and COP. This simulation model gave clear figures to evaluate the performance of the ACS and suggested useful method to improve the design of the adsorber. This simulation model will be employed in future study and will be modified to simulate the adsorber with more complex geometry in order to find out the achievable system COP and SCP of ACS.

ACKNOWLEDGMENTS

Funding for this study was provided by the Hong Kong PhD Fellowship Scheme (HKPFS).

REFERENCES

[1] E.I.A., International Energy Statistics, 1988 – 2008, U.S. Energy Information Administration, accessed on 23/6/2011, http://www.eia.gov/cfapps/ipdbproject/IEDIndex3.cfm.

[2] U.S. Energy Information Administration, E.I.A., Regional Energy Profile: U.S. Household Electricity Report (2005).

[3] U.S. Energy Information Administration, E.I.A., Trends in Residential Air-Conditioning Usage from 1978 to 1997 (2000).

[4] Hong Kong Government, Hong Kong Energy End-use Data 2010, Electrical & Mechanical Services Department (2010).

[5] R.Z. Wang and R.G. Oliveira, Adsorption refrigeration: An efficient way to make good use of waste heat and solar energy, Prog. Energ. Combust. 32 (2006) 424–458.

[6] D.S. Kim, C.A.I. Ferreira, Solar refrigeration options: A state-of-the-art review, Int. J. Refrig. 31 (2008) 3–15.

[7] E.E. Anyanwu, N.V. Ogueke, Thermodynamic design procedure for solid adsorption solar refrigerator, Renew. Energ. 30 (2005) 81–96.

[8] H. Demir, M. Mobedi, S. Ülkü, A review on adsorption heat pumps: Problems and solutions, Renew. Sust. Energ. Rev. 12 (2008) 2381–2403.

[9] R.Z. Wang, T.S. Ge, C.J. Chen, Q. Ma, Z.Q. Xiong, Solar sorption cooling systems for residential application: Options and guidelines, Int. J. Refrig. 32 (2009) 638–660.

[10] D.I. Tchernev, D.T. Emerson, High-efficiency regenerative zeolite heat pump, ASHRAE T. 14 (1988) 2024–2032.

[11] K.C. Chan, C.Y.H. Chao, G.N. Sze-To, K.S. Hui, Performance predictions for a new zeolite 13X/$CaCl_2$ composite adsorbent for adsorption cooling systems, Int. J. Heat Mass Tran., CT11-137, accepted

[12] M. Pons, P. Grenier, A phenomenological adsorption equilibrium law extracted from experimental and theoretical considerations applied to the active carbon + methanol pair, Carbon 24 (1986) 615–625.

[13] D.C. Wang, Z.Z. Xia, J.Y. Wu, Design and performance prediction of a novel zeolite–water adsorption air conditioner, Energ. Convers. Manage. 47 (2006) 590–610.

[14] D.M. Ruthven, Fundamental of adsorption equilibrium and kinetics in microporous solids, Mol. Sieves 7 (2008) 1–43.

[15] D. Ko, R. Siriwardane, L.T. Biegler, Optimization of a Pressure-Swing Adsorption Process Using Zeolite 13X for CO_2 Sequestration, Ind. Eng. Chem. Res. 42 (2002) 339–348.

[16] S.J. Gregg, K.S.W. Sing, Adsorption, surface area, and porosity, Academic Press, London, New York (1967) 371.

[17] S. Dini, W.M. Worek, Sorption Equilibrium of a Solid Desiccant Felt and the Effect of Sorption Properties on a Cooled-Bed Desiccant Cooling System, Journal of Heat Recovery Systems, 6 (1986) 151-167.

[18] B.B. Saha, A. Chakraborty, S. Koyama, Y.I. Aristov, A new generation cooling device employing $CaCl_2$-in-silica-gel-water system, Int. J. Heat Mass Tran. 52 (2009) 516–524.

[19] N.B. Amar, L.M. Sun, F. Meunier, Numerical analysis of adsorptive temperature wave regenerative heat pump, Appl. Therm. Eng. 16 (1996) 405–418.

[20] K. Asano, Mass transfer: From fundamentals to modern industrial applications, Wiley-VCH, (2006).

[21] K.C. Leong, Y. Liu, System performance of a combined heat and mass recovery adsorption cooling cycle: A parametric study, Int. J. Heat Mass Tran. 49 (2006) 2703–2711.

[22] C.T. Hsu, P. Cheng, K.W. Wong, Modified Zehner-Schlunder models for stagnant thermal conductivity of porous media, Int. J. Heat Mass Tran. 37 (1994) 2751–2759.

[23] M.B. Cutlip, M. Shacham, Problem solving in chemical and biochemical engineering with POLYMATH, Excel, and MATLAB, Prentice Hall, (2008)

[24] J.C. Tannehill, D.A. Anderson, R.H. Pletcher, Computational fluid mechanics and heat transfer, McGraw-Hill : Hemisphere Publising Co., NY (1984).

[25] G. Restuccia, A. Freni, S. Vasta, Yu.I. Aristov, Selective water sorbent for solid sorption chiller: Experimental results and modeling, Int. J. Refrig. 27 (2004) 284–293.

[26] X.J. Zhang, K. Sumathy, Y.J. Dai, R.Z. Wang, Dynamic hygroscopic effect of the composite material used in desiccant rotary wheel, Sol. Energy 80 (2006) 1058–61.

[27] Z. Han, A. Fina, Thermal conductivity of carbon nanotubes and their polymer nanocomposites: A review, Progress in Polymer Science 36 (2011) 914-944.

[28] S.P. Hepplestone, A.M. Ciavarella, C. Janke, G.P. Srivastava, Size and temperature dependence of the specific heat capacity of carbon nanotubes, Surface Science 600 (2006) 3633-3636.

[29] A. Striolo, P.K. Naicker, A.A. Chialvo, P.T. Cummings, K.E. Gubbins, Simulated water adsorption isotherms in hydrophilic and hydrophobic cylindrical nanopores, Adsorption 11 (2005) 397-401.

[30] A. Striolo, A.A. Chialvo, K.E. Gubbins, P.T. Cummings, Water in carbon nanotubes: Adsorption isotherms and thermodynamic properties from molecular simulation, The Journal of Chemical Physics 122 (2005) 234712.